Journal Pre-proofs

Regular Article

Biomimetic core-shell silica nanoparticles using a dual-functional peptide

Tengjisi, Yue Hui, Guangze Yang, Changkui Fu, Yun Liu, Chun-Xia Zhao

PII: S0021-9797(20)30989-9
DOI: https://doi.org/10.1016/j.jcis.2020.07.107
Reference: YJCIS 26731

To appear in: *Journal of Colloid and Interface Science*

Received Date: 22 May 2020
Revised Date: 10 July 2020
Accepted Date: 22 July 2020

Please cite this article as: Tengjisi, Y. Hui, G. Yang, C. Fu, Y. Liu, C-X. Zhao, Biomimetic core-shell silica nanoparticles using a dual-functional peptide, *Journal of Colloid and Interface Science* (2020), doi: https://doi.org/10.1016/j.jcis.2020.07.107

Biomimetic core-shell silica nanoparticles using a dual-functional peptide

Tengjisi, Yue Hui, Guangze Yang, Changkui Fu, Yun Liu, Chun-Xia Zhao*

Australian Institute for Bioengineering and Nanotechnology, University of Queensland, St. Lucia, Queensland 4072, Australia.

*e-mail: z.chunxia@uq.edu.au (C.-X.Z.)

Abstract

Biomimetic nanomaterials have attracted tremendous research interest in the past decade. We recently developed biomimetic core-shell nanoparticles – silica nanocapsules, using a designer dual-functional peptide SurSi under room temperature, neutral pH and without use of any toxic reagents or chemicals. The SurSi peptide is designed capable of not only stabilizing nanoemulsions because of its excellent surface activity, but also inducing the formation of silica through biosilicification at an oil-water interface. However, it remains challenging to precisely control the peptide-induced nucleation and biosilicification specifically at the oil-water interface, thus forming oil-core silica-shell nanocapsules with uniform size and monodispersity. In this study, the fundamental mechanism of silica formation through a peptide catalyzed biosilicification was systematically investigated, so that the formation of oil-core silica-shell nanocapsules can be precisely controlled. The SurSi peptide induced hydrolysis and nucleation of biomineralized silica particles were monitored to study the biosilicification kinetics. Effects of pH, SurSi peptide concentration and pre-hydrolysis of silica precursors were also studied to optimize the formation of biomimetic silica nanocapsules. The fundamental understanding achieved through these systematic studies provides valuable insights for making core-shell nanoparticles via controlling nucleation and reaction at interfaces.

Introduction

Core-shell nanoparticles are attractive as the core can be loaded with drug or image agents, and the shell provides a barrier protecting the loaded active components as well as makes it easier for different surface modification [1]. The choice of material for the core and shell affect greatly their final applications [2]. Depending on the selection of the shell materials, methods for making core-shell nanoparticles are diverse [2, 3], such as precipitation [4-6], polymerization

[7-10], microemulsion[11-13], sol-gel condensation [14, 15], and layer by layer adsorption techniques [16, 17].

Silica is an attractive shell material. It provides many advantages including good biocompatibility and degradability, good dispersity, and easy to functionalize [18, 19]. Traditional methods for making silica core-shell materials are mainly based on the sol-gel method that often requires toxic chemicals or solvents, high temperature or extreme pH to remove the core, which could result in toxic residues in the final materials, inconsistent shell structure or rupture of the shell because of the harsh conditions used for core removal. In contrast, biomimetic mineralization has attracted significant interests in making various kind of inorganic nanomaterials such as silica, titania [20], calcium phosphate [19], metal organic frameworks (MOFs) [21, 22] owning to its benign synthesis conditions.

We developed a novel and green biomimetic technology to form core-shell materials using dual-functional peptides [23-29]. These biomolecules have a unique two-module design, one module for surface activity to make stable droplets, and the other one for biosilisification activity. Briefly, oil-in-water emulsions are formed by dispersing oil in an aqueous solution containing the dual-module peptide. Because of the excellent surface activity of this peptide, monodisperse emulsions can be formed with the peptide adsorbing at the interface [30]. Then a silica precursor (e.g., tetraethyl orthosilicate, TEOS) is added to the emulsion to initiate the biosilicification at the oil-water interface at room temperature, neutral pH, and without toxic chemicals or reagents. After mixing, silica nanocapsules are generated with a well-controlled core-shell structure. The core size, which depends on the droplet size, can be tuned by using different homogenization energy input, different concentrations of peptide or different volume ratio of the oil phase, while the shell thickness can be controlled by adjusting the reaction time and the precursor concentration[25]. This bioinspired method is simple, sustainable, biocompatible, and doesn't involve any extreme conditions or toxic chemicals. It offers a unique strategy for making functional core-shell materials for various applications [1]. However, the mechanism underlying the silica hydrolysis, nucleation, growth mediated by the biomolecule remains unclear.

In this study, we systematically investigate the hydrolysis, nucleation and growth of silica, the composition of the silica nanoparticles based on biosilicification using a peptide, as well as the effect of pH, pre-hydrolysis on the formation of core-shell nanoparticles. This study provides

a comprehensive understanding of the biomolecule directed silica formation at oil-water interfaces.

Experimental

Materials. Materials. Peptide SurSi (Ac-MKQLAHSVSRLEHA RKKRKKRKKRKKGGGY-$CONH_2$) was synthesized by Mimotopes Pty Ltd. (Australia) with a purity ≥95%. Water having resistivity >18.2 MΩ·cm was obtained from a Milli-Q system (Millipore, Australia) equipped with a 0.22 μm filter. Tetraethoxysilane (TEOS), zinc chloride ($ZnCl_2$), ammonia, and 4-(2-hydroxyethyl)-1-piperazineethanesulfonic acid (HEPES) were of analytical grade purchased from Sigma-Aldrich and used as received unless otherwise stated.

Silica nanoparticle formation by biosilicification. Silica nanoparticles were synthesized based on a biosilicification method using a designer peptide SurSi. Tetraethoxysilane (TEOS, 10, 40 or 80 mM) and SurSi (200 μM) were mixed in 25 mM HEPES buffer at pH 7.5 under 350 rpm magnetic stirring at room temperature (25 °C). The reaction was monitored over a period of 42 hours. Dynamic Light Scattering (DLS) was used to monitor the reaction. At different time points of 11, 14, 16, 17, 18, 19, 20, 21, 24, 27, 30, 33, 36, 39, and 42 h, the sample was analyzed using DLS (size, polydispersity index, derived count rates and zeta potential). To study the effect of TEOS concentration on silica nanoparticle morphology, 5 μL sample was taken for Transmission Electron Microscopy (TEM) observation at 18, 24, 36 and 42 h. To study the effect of pH on biosilication, HEPES buffer with pH ranging from 6.5 to 8.5 (HEPES buffer range: pH=6.8 to 8.2) was prepared for reaction, and 5 μL sample was collected for TEM observation at 18, 24 and 40 h.

Silica nanoparticles formation by Stöber method. Silica particles were also prepared by the Stöber method [31]. 2.39 mL ethanol, 106.5 μL ammonium hydroxide and 325.7 μL water were mixed under 500 rpm magnetic stirring at room temperature for 45 min, then 175.4 μL TEOS was added and reacted for another 80 min.

Trifluoroacetic acid (TFA) removal. SurSi peptide was dissolved in Milli-Q water and then dialysis with 3.5 kDa cutoff Snakeskin membrane (Thermo Fisher Scientific) in 1L Milli-Q water at 4 ºC overnight to remove TFA. Then SurSi without TFA was lyophilized and quantified using High Performance Liquid Chromatography (HPLC) for biosilicification.

Silica nanocapsule synthesis using SurSi. To make nanoemulsions, SurSi peptide was dissolved in HEPES buffer (25 mM, pH 7) to prepare a peptide solution of 400 μM, followed by adding 800 μM $ZnCl_2$. Miglyol 812 oil (2% v/v) was added to the peptide solutions. For 3 mL emulsion, 60 μL Miglyol 812 oil was added into 2940 μL peptide solution. The peptide solution was sonicated using a Sonifier 450 ultrasonicator (Branson Ultrasonics, Danbury, CT) for 30 seconds five times with 1 min cooling between each sonication. The nanoemulsion was dialysed using 10 kDa cutoff Snakeskin membrane (Thermo Fisher Scientific) in 25 mM, pH=7.5 HEPES buffer at 4 ºC for certain time (5-20 h). Silica precursor tetraethoxysilane (TEOS) was added and reacted with nanoemulsion at room temperature. Nanocapsules were dialysed in 25 mM pH=7.5 HEPES buffer at 4 ºC for 16 h to remove residual peptide and stop the reaction. To investigate the effect of pre-hydrolysis on silica capsules formation, silica precursor was hydrolyzed in 500 μL of 200 μM SurSi solution for 6 and 10 hours, then mixed with 500 μL emulsion to make silica nanocapsules.

Interfacial tension. Interfacial tension was measured by a Drop shape analysis DSA-10 method (Krüss GmbH, Germany). To measure interfacial tension kinetics, a quartz cuvette (Hellma GmbH, Germany) was filled with a peptide solution sample (8 mL) of SurSi in HEPES buffer (25 mM, pH 11). A Miglyol 812 oil droplet was formed in the peptide solution through an inverted stainless-steel needle with a diameter of 1.507 mm connected to a glass syringe. The instrument was calibrated by forming a pure oil droplet (Miglyol 812) in HEPES buffer without peptide, confirming a constant interfacial tension of approximately 30 mN/m. The interfacial tension was measured automatically over 600 s after the initial formation of an oil droplet.

Characterizations

Dynamic Light Scattering (DLS). The size, polydispersity index (PdI) and zeta potential of the silica nanoparticles were measured by Malvern Zetasizer Nano ZS (Malvern Instruments, Malvern, UK). The scattering angle of measurement was 173° and the measurement was set at room temperature 25 °C.

Transmission Electron Microscopy (TEM). The morphologies of silica nanoparticles were imaged by Hitachi HT7700 transmission electron microscopy (Hitachi, Tokyo, Japan) under 100 kV voltage. To prepare the TEM samples, 5 μL silica nanoparticle solution was pipetted from the bulk solution and dropped onto a formvar-coated copper grid. After 5 min drying, extra liquid was absorbed by Kimtech wipes (Kimberly Clark, Irving, Texas, US).

Fourier-transform infrared (FTIR). The surface chemical structure was determined by Fourier-transform infrared (FTIR) spectroscopy. Nanoparticles were lyophilized into dry powder and analysed by using a Nicolet™ iS50 FTIR Spectrometer (Thermo Fisher Scientific, Waltham, MA).

Thermogravimetric analysis (TGA). The peptide content in silica particles were determined by thermogravimetric analysis (TGA) using a STARe thermogravimetric analyzer (Mettler-Toledo, LLC, Columbus, OH). Particles were washed three times with water to remove residual chemicals and peptide, then lyophilized for TGA analysis. Samples were heated from 40 to 950 °C at a rate of 10 °C min^{-1}.

Data analysis. All the experiments were performed in triplicate and repeated three times, and average of the results were used to make the plots or tables.

Results

Formation of bioinspired silica nanocapsules

The biomimetic approach for making oil-core silica-shell nanocapsules is a simple emulsion-templated biosilicification method using a bifunctional peptide SurSi (Ac-MKQLAHSVSRLEHA RKKRKKRKKRKKGGGY-$CONH_2$). **Fig. 1** shows the process for synthesizing silica nanocapsules. Typically, the SurSi peptide is dissolved in a HEPES buffer to make a peptide solution, and 2% v/v Miglyol 812 oil is added to the peptide solution, followed by sonication to make nanoemulsions. Then, the nanoemulsion is dialyzed to reduce the free peptide in the bulk solution to avoid the formation of silica particles in the bulk solution. A silica precursor is then added to the nanoemulsion to initiate the reaction. After reacting for a certain period of time under stirring, the suspension is dialyzed to remove residual silicic acid and stop the reaction, and silica nanocapsules are synthesized. Although it is a simple and facile process, the precise control of biosilicification specifically at oil-water interface rather than in bulk solution thus forming uniform oil-core silica-shell nanoparticles is not trivial. Therefore, it is important to fundamentally understand the peptide-mediated nucleation and growth of silica in the presence of oil-water nanoemulsions.

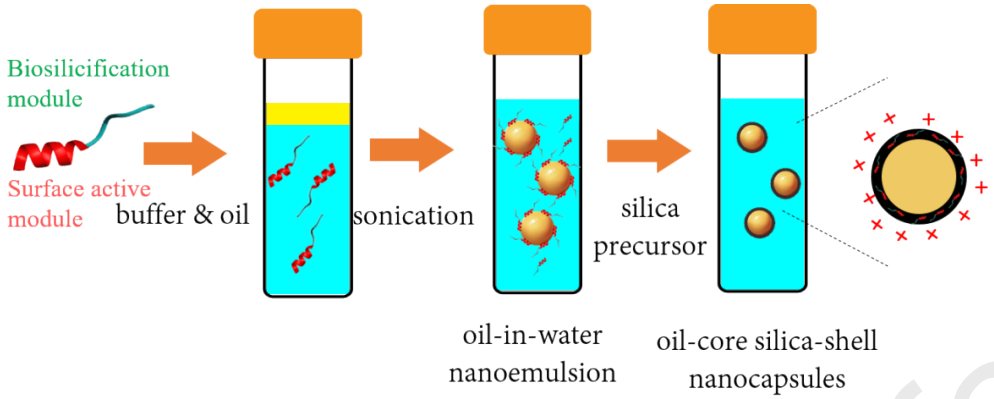

Fig. 1. Schematic of emulsion-templated silica nanocapsule formation.

Effect of silica precursor concentration on nucleation and growth of silica nanoparticles

To investigate the peptide catalyzed nucleation and growth of silica via the sol-gel process, 200 µM SurSi was mixed with TEOS of different concentrations (10, 40 and 80 mM), and the reaction was monitored using DLS, including particle size, polydispersity index (PDI), derived count rate (DCR) and zeta potential (**Fig. 2**). The peptide catalyzed biosilicification started with the hydrolysis of TEOS, so no particle was detected in the first 15 hours (**Fig. 2a**). Then the sudden increase of particle size and PDI at 16-20 h for 40 and 80 mM TEOS indicated a sol-to-gel transition forming three-dimensional siloxane network [32]. For a very low concentration of 10 mM TEOS, it didn't show the dramatic size increase until 21 h due to the low concentration of hydrolyzed silicic acid, as nucleation only occurs after the hydrolysed silicic acid concentration reaches the critical homogenous nucleation concentration [33]. For higher TEOS concentrations (40 and 80 mM), it took another 6-7 hours for the particle size to stabilize at around 100 nm to 150 nm, whereas this condensation process was much longer (around 14 hours) for 10 mM TEOS. Also, it was obvious that the resultant silica nanoparticle size decreased with TEOS concentration. After 36 hour reaction, the silica nanoparticle sizes were 107.4 nm, 124.1 nm and 136.8 nm for 10 mM, 40 mM and 80 mM TEOS, respectively.

Fig. 2b shows the polydispersity index (PDI) results reflecting the dispersity of particles suspension. Similar to the particle size result, there was a big jump at around 18 h for 40 and 80 mM TEOS and 24 h for 10 mM TEOS, indicating the formation of irregular three-dimensional siloxane network. Then when silica nanoparticles started to form, the PDI decreased and remained stable at around 0.2 (for 10 and 40 mM TEOS) indicating the formation of uniform silica nanoparticles. It was also observed that higher TEOS concentration led to quicker particle growth, resulting in higher chance of aggregation. As a result, the 80 mM

TEOS generated nanoparticles with slightly higher PDI (~0.3) than those using 10 and 40 mM TEOS.

Derived count rate (DCR) is the count rate divided by the attenuation factor, which has a positive correlation with the particle number in the solution. Nucleation results in rapid and distinct growth in particle number where DCR increases rapidly. As shown in **Fig. 2c**, the DCR increased significantly between 18 hours to 21 hours for 40 and 80 mM TEOS indicating the start of nucleation. After initial nucleation at 18 h, the particles number kept growing until 36 h and remained constant at 36-42 h, which is consistent with the result of particle size (**Fig. 2a**). This indicates that nucleation occurs mainly during 18-36 h, followed by particle growth at 36-42 h. **Fig. 2c** also shows the effect of TEOS concentration on nucleation and particle growth. Higher TEOS concentrations (40 mM and 80 mM) generated higher nucleation rate and more particles in the solution compared to lower TEOS concentration (10 mM). Similar to the size and PDI results, the DCR increase of 10 mM TEOS was also delayed about 9 hours, and the final DCR number was much lower than those of the 40 and 80 mM TEOS reactions.

Fig. 2d shows the surface charge of the particles. Nuclei formed at the beginning with slightly negative charges. But when silica nanoparticles started to form, their zeta potential increased significantly to +15-20 mV suggesting the adsorption of positively charged peptide SurSi on the negatively charged silanol groups, which is in contrast to silica formation using chemical methods. Then after peptides were consumed, the zeta potential of silica particles decreased and the particles start to aggregate. Consequently, the PDI of the particles started to grow after 40 hours, and big aggregation formed with even longer reaction time (e.g. 50 hours). Again, the zeta potential change of silica nanoparticles using 10 mM TEOS occurred much later (at around 40 h).

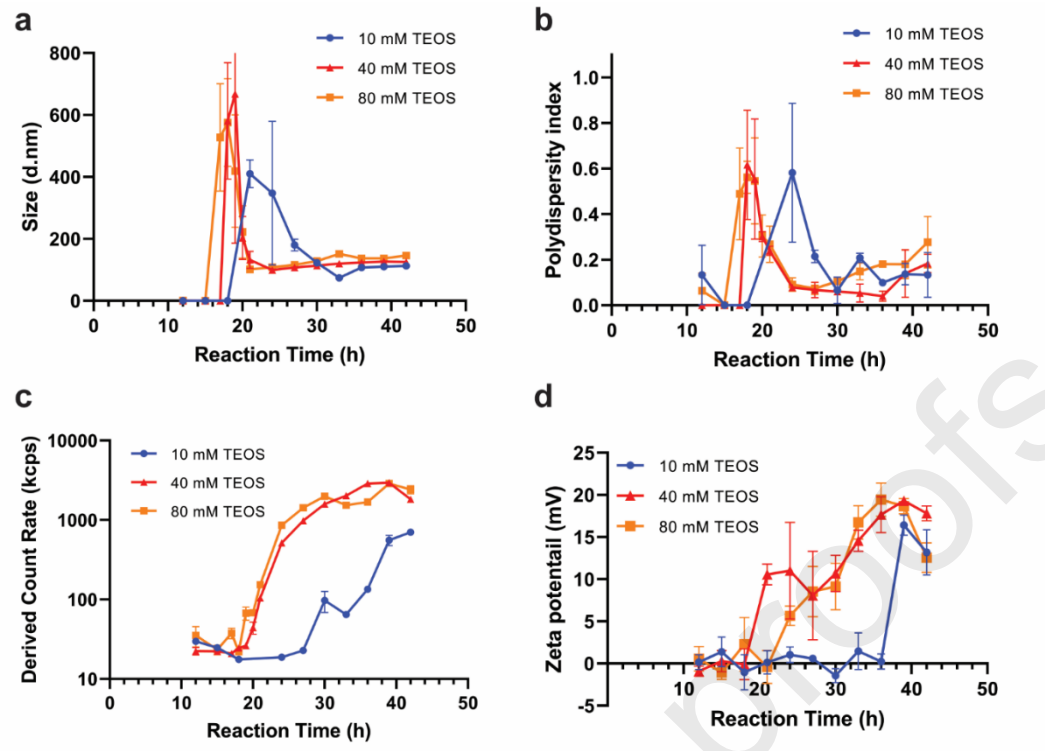

Fig. 2. Dynamic Light Scattering results of nucleation and particle growth during SurSi peptide induced biosilicification (TEOS reacted with 200 µM SurSi in 25 mM pH 7.5 HEPES buffer)**. a**, Silica nanoparticles size in diameter; **b**, PDI; **c**, Derived count rate; **d**, Zeta potential.

These DLS results depict the peptide catalyzed nucleation and growth of silica via a sol-gel process. The concentration of silica precursor TEOS affected significantly the hydrolysis and condensation of TEOS, consequently the nucleation and growth of silica with a big delay for a low TEOS concentration (10 mM), while there was not much difference between 40 amd 80 mM TEOS. For these two higher concentrations, an induction time of about 15 hours was observed suggesting the hydrolysis of TEOS and formation of a sol solution. Then the sol solution was converted to a gel with a three-dimensional network accompanied by a sudden size jump. Then after 6-7 h polymerization and condensation, uniform silica nanoparticles were generated. While further prolonging the reaction resulted in bigger particle size and slightly increased PDI. Surprisingly, these peptide-induced silica nanoparticles had positive charges indicating the incorporation of positively charged SurSi peptide.

Silica particle morphology was observed using TEM **(Fig. 3),** showing the formation of a few irregular nuclei at 18 h. Then many small particles with size ranging from 20 nm to 50 nm were observed at 24 h. Higher silica precursor concentration resulted in higher nucleation rate so produced more and bigger particles. With longer reaction time, silica nanoparticles became

denser and larger. At 42 h, many particles with sizes around 100 nm were formed with spherical shape. The concentration of TEOS didn't have much effect on the final silica particle size.

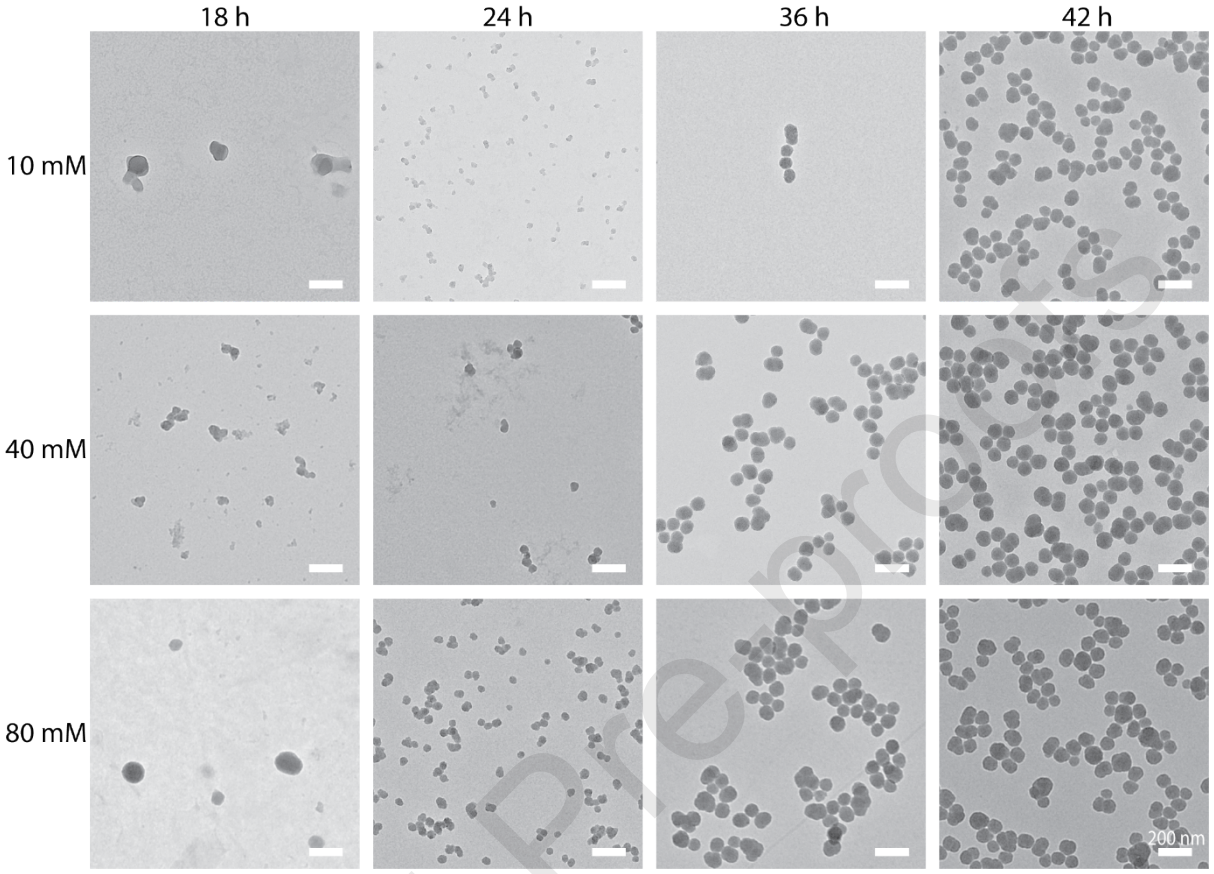

Fig. 3. TEM image of TEOS silica particles. 10 mM, 40 mM, 80 mM TEOS reacted with 200 μM SurSi in 25 mM pH 7.5 HEPES buffer from 18 h to 42 h, the scale bars are 200 nm.

Effect of SurSi peptides on silica nanoparticles

As mentioned above, the SurSi-induced silica nanoparticles showed distinct charge from traditional silica nanoparticles. To determine the role of the SurSi peptide in biosilicification and the amount of peptides contained in the nanoparticles, silica nanoparticles prepared by biosilicification were compared to those synthesized using the Stöber method. Although the Stöber method produced silica nanoparticles (**Table 1)** with a similar size (149.4 nm) as those silica nanoparticles by biosilicification (145.1 nm), their surface charges were distinct. The Stöber silica nanoparticles was negative, while the bioinspired silica was positively charged indicating the presence of the SurSi peptide in the particle. As shown in **Fig.4**, both bioinspired silica nanoparticles and Stöber silica nanoparticles were amorphous, but the Stöber silica nanoparticles have a more smooth surface than the bioinspired silica (**Fig. 4b, 4d**).

To further confirm the presence of SurSi in the bioinspired silica nanoparticles, FTIR study was conducted for both the Stöber silica and bioinspired silica. **Fig. 5a** shows that both Stöber silica and bioinspired silica had the peak around 1650 cm^{-1} which corresponds to the signal of the N-H bond from either arginine (R) and lysine (K) in the peptides or the ammonium hydroxide used in the Stöber method. After washing, most of ammonium was removed, so N-H bonding in bioinspired silica was much stronger. Biomimetic silica also showed a very strong peak at 1540 cm^{-1} (corresponding to C-H bending) suggesting again the presence of SurSi peptide in the biomimetic silica nanoparticles.

Table 1. DLS results for silica nanoparticles prepared by biosilicification method and Stöber method.

Sample	Size (d.nm)	PDI	Zeta potential (mV)
Bioinspired silica nanoparticles	145±1	0.28±0.01	18.7±0.8
Stöber silica nanoparticles	150±1	0.06±0.01	-40.2±0.5

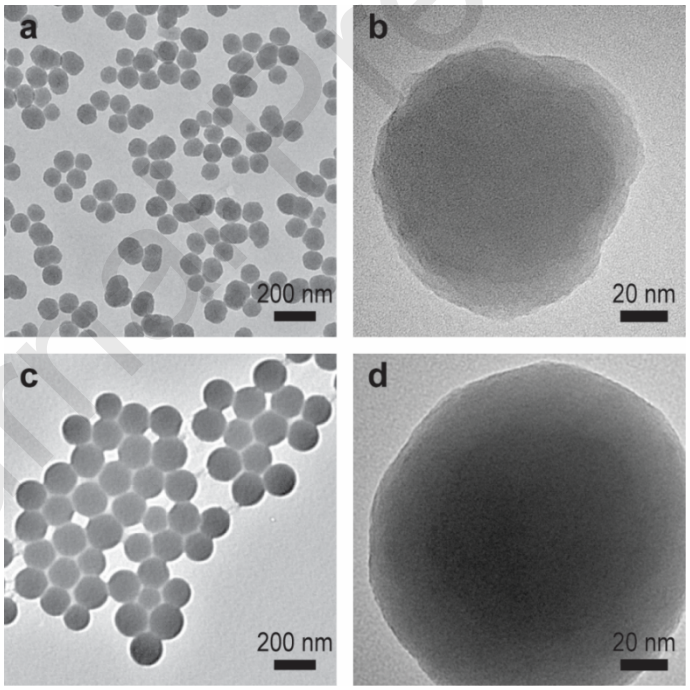

Fig. 4. TEM image of silica particles. a, b. Biomimetic silica nanoparticles (40 mM TEOS reacted with 200 µM SurSi in 25 mM pH 7.5 HEPES buffer from 42 h), **c, d.** Stöber silica nanoparticles. The scale bars are 200 nm.

To quantify the amount of peptide in the silica nanoparticles, thermal gravimetric analysis (TGA) was conducted using the Stöber silica particles as the reference. As shown in the **Fig.**

5b silica particles kept losing weight with the increasing of temperature. The weight loss at around 100 ºC was water residual that was not removed through lyophilisation. After 100 ºC, the Stöber silica nanoparticles lost weight slowly mainly from the further condensation of hydroxyl group under high temperature. For bioinspired silica nanoparticles, from 100 ºC to 500 ºC, the weight loss of the silica nanoparticles was not only from condensation of hydroxyl group but also from the burned peptide, which were around 18 % (Table 2). In contrast, the Stöber silica nanoparticles had 7.1% weight loss and the SurSi peptide lost 80% weight from 100 – 500°C. The residual 12% weight of the SurSi peptide was mainly from salts contained in the sample. The significant weight loss of the bioinspired silica nanoparticles (18%) in contrast to that of the Stöber silica (7.1%) confirmed the presence of SurSi peptide in the particles.

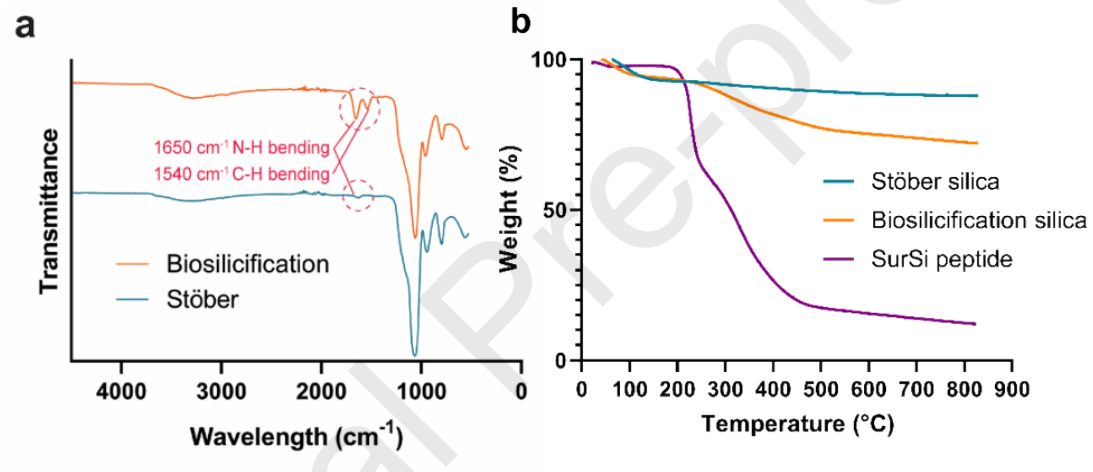

Fig. 5. Fourier-transform infrared spectroscopy spectrum (a) and TGA results (b) of the silica nanoparticles formed by biosilicification and the Stöber method. Orange: silica particles prepared by biosilicification method; Cyan: silica particles prepared by the Stöber method; Purple: SurSi peptide.

Table 2 Percentage of weight loss versus temperature

Sample	Percentage of weight loss %		
	25-100°C	100-500°C	500-800°
Stöber silica	3.6	7.1	1.4
Biosilificiation silica	4.8	18.1	4.7
SurSi peptide	2.2	80.3	5.1

Effect of trifluoroacetic acid (TFA) on peptide activity

TFA or TFA salt often presents in the commercial peptide product. Thus, it is important to investigate whether TFA affects the peptide activity during biosilicification. In biosilicification, both the surface activity from Sur module and the ability to induce silica formation from Si mudule are important, so two questions need to be answered (i) whether TFA affects the surface activity of SurSi; (ii) whether TFA affects silica formation. To address the first question, the interfacial tension of Miglyol 812 oil in SurSi peptide solution with and without TFA were measured at pH=11 (**Fig. 6)**. Both SurSi with and without TFA had strong surface activity, but SurSi with TFA showed a slightly lower interfacial tension of 6.04 mN/m. As TFA is slightly surface active, it can adsorb on interface which could affect silica shell formation. As shown in **Fig. 7**, the silica shell formed by SurSi with TFA was thinner than that from SurSi without TFA. The silica shell thickness formed without TFA was around 25 nm in average, and the shell was more even. In contrast, the silica shell synthesized using SurSi with TFA were only 20 nm for the thickest part, and for the thinnest area, the shell thickness was less than 8 nm, which makes the shell prone to break. Therefore, it is very important to remove TFA from the peptide sample.

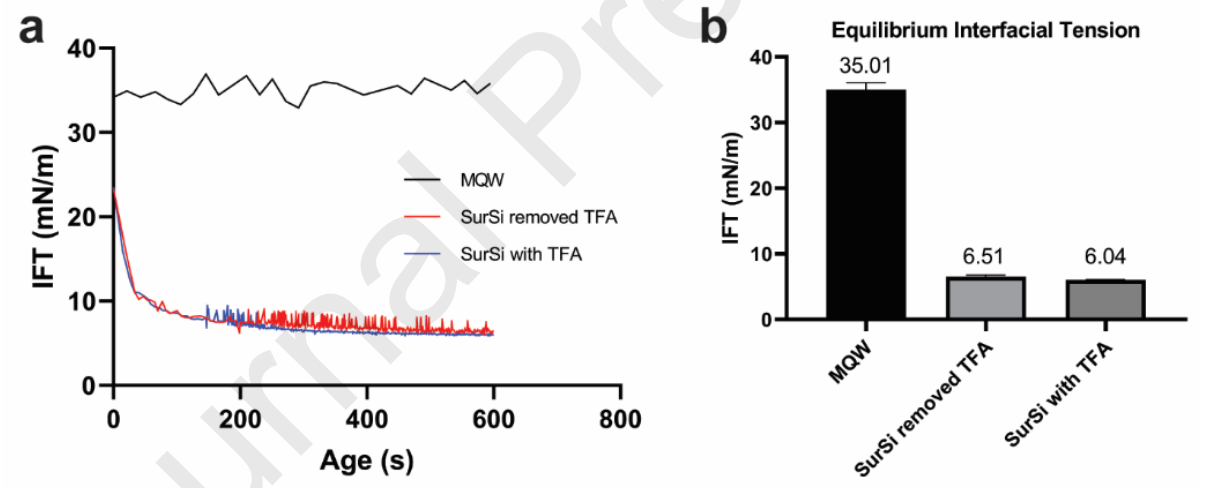

Fig. 6 Effect of TFA on peptide surface activity. a. Interfacial tension of Miglyol 812 in **black:** Milli-Q water, **Red:** SurSi peptide dialysed for 16 hours to remove TFA, SurSi concentration was 200 µM, **Blue:** SurSi peptide with TFA, SurSi concentration was 200 µM, TFA content was 43.5% according to the synthesis report, TFA concentration was 4.9 mM. The pH of three solutions were adjusted to 11 by NaOH; **b:** Equilibrium interfacial tension.

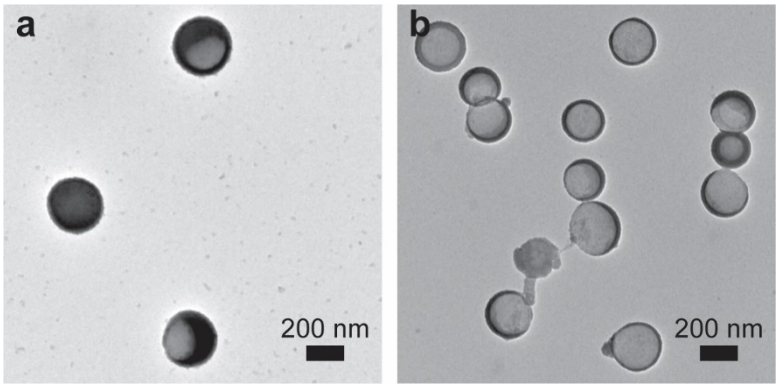

Fig. 7 TEM image for TEOS silica nanocapsules: **a.** 200 μM SurSi peptide without TFA **b.** 200 μM SurSi with 4.9 mM TFA. Reaction was carried out in 25 mM HEPES buffer (pH=7.5) for 30 hours. The scale bars are 200 nm.

Effect of pH and peptide concentration on biosilicification

In order to investigate the effect of pH on biosilicification, silica particle formation was monitored under different pH (from 6.5 to 8.5). The chemical reactions during the sol-gel process can be described by the following three equations:

$$\equiv Si - OR + H_2O \rightarrow \equiv Si - OH + ROH \quad \text{Hydrolysis} \quad (1)$$

$$\equiv Si - OH + Si - OR \rightarrow \equiv Si - O - Si \equiv + ROH \quad \text{Condensation} \quad (2)$$

$$\equiv Si - OH + \equiv Si - OH \rightarrow \equiv Si - O - Si \equiv + H_2O \quad \text{Condensation} \quad (3)$$

pH as the catalyst affects the reaction mechanisms for acid or base catalysis very differently. The minimum rate for hydrolysis is at pH 7, for condensation at pH 4.5 [34]. Therefore, either very low or very high pH in the presence of solvents (ethanol, methanol, etc.) is used for making silica particles. In contrast, we developed this SurSi-induced biosilicification approach under near neutral pH and without any solvents. But the pH effect on hydrolysis and condensation also applies for our biosilicification. In addition to the peptide SurSi, pH also acts as a catalyst, so when pH is reduced to below 7, the condensation is compromised, but pH above 7 not only increases the hydrolysis but also the condensation, and too high pH makes the reaction too rapid thus uncontrolled formation of silica. This agrees with what we observed in the experiments. As shown in **Fig. 8**, lower pH led to much slower reaction rate, so no particle was detected and observed. Higher pH gave much more rapid hydrolysis rate, and the peptide activity was also higher, which made the reaction very fast. At pH=8.0, large particles appeared within 18 hours, and after 40 hours huge aggregation was observed. Therefore pH 7.5 was selected for forming silica.

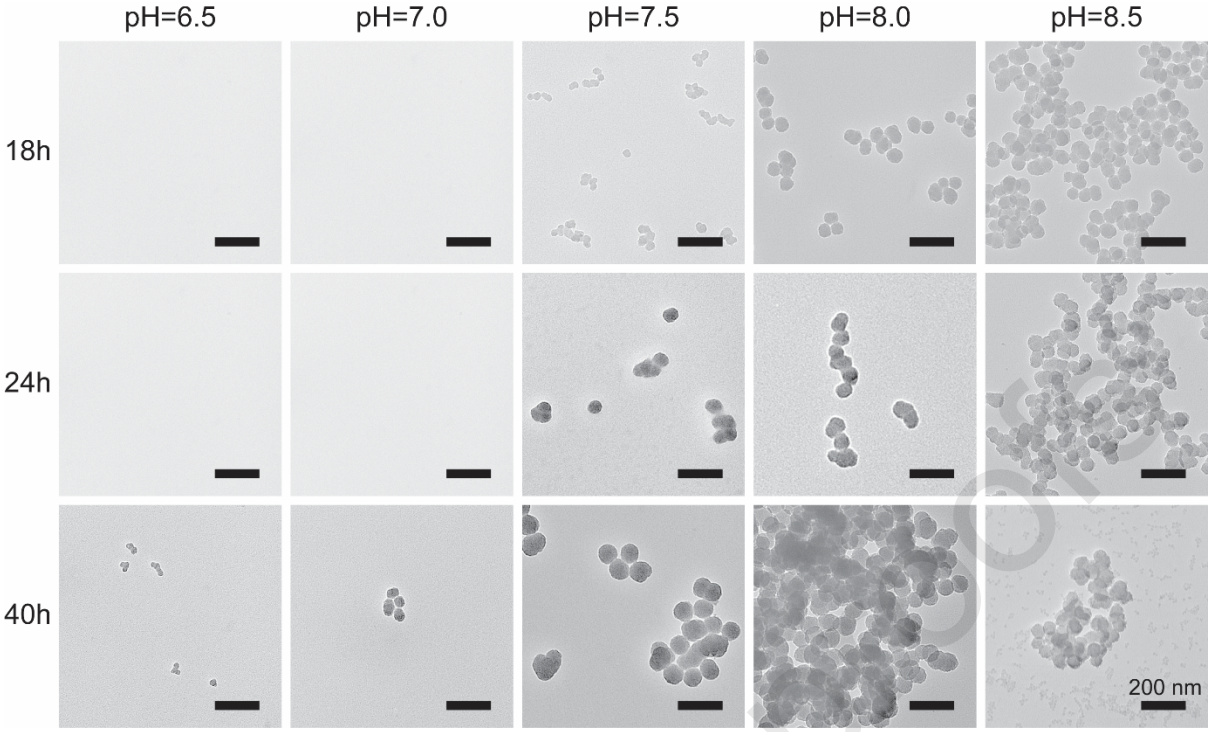

Fig.8 Effect of pH on biosilicification. Reaction time was 18, 24 and 40 hours and the pH ranged from 6.5 to 8.5. The scale bars are 200 nm.

The peptide concentration also plays an important role. Higher nucleation rate was observed when increasing the SurSi concentration from 100 to 400 μM resulting in smaller particles (**Fig. 9**). But high peptide concentration could also lead to the formation of silica particles in the bulk solution rather than on the oil-water interface to form silica nanocapsules.

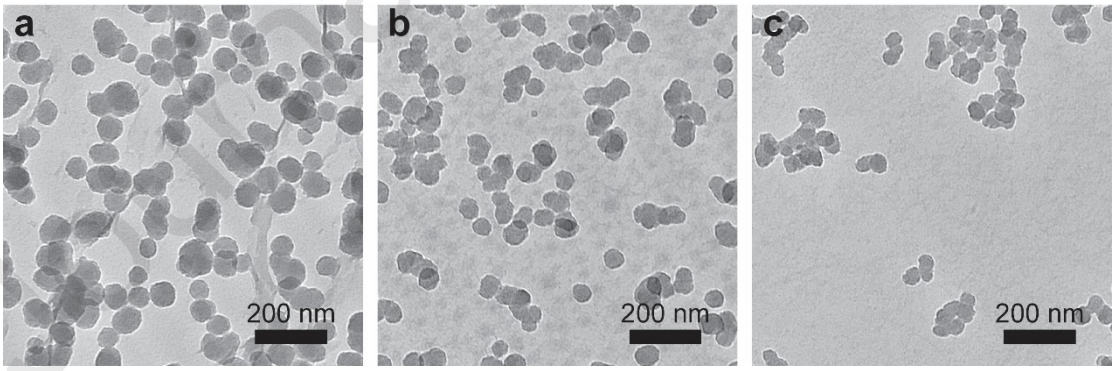

Fig.9 Effect of SurSi concentration on biosilicification. **a.** 100 μM; **b.** 200 μM and **c.** 400 μM. Reaction time was 24 hours. The scale bars are 200 nm.

The effect of SurSi concentration in the bulk solution on nanocapsule formation was investigated by dialyzing the emulsion for different time including 5, 10, 20, 22 h, and the residual SurSi concentrations in the bulk solution were 167, 146, 101 and 97 μM, respectively.

We found that uniform nanocapsules were produced for 5-20 hours dialysis time, which corresponds to peptide concentrations around 100 – 167 μM (**Fig. 10**). Shorter dialysis time led to precipitation of silica nanoparticles in the bulk solution, while longer dialysis resulted in slower biosilicification and no formation of nanocapsules of good quality.

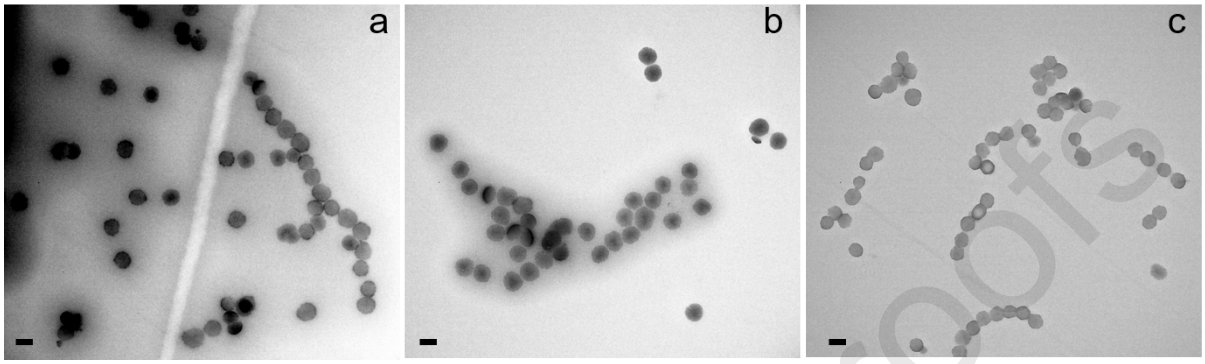

Fig.10 Effect of dialysis time on nanocapsule formation. a: 5 h dialysis; b: 10 h dialysis; c: 20 h dialysis. Reaction time was 30 h. The scale bars are 200 nm.

Effect of silica precursor pre-hydrolysis on silica capsules formation. To further study the mechanism of silica nanocapsules formation, whether the nanocapsule formation requires hydrolysing around the emulsion droplets, or silicic acid could hydrolyze first and then adsorb onto the emulsion droplets surface to form silica shell, pre-hydrolysis of the silica precursor TEOS was introduced to the experiment (Table 3). 40 mM TEOS was hydrolyzed in the presence of 200 μM SurSi for 6 or 10 hours, then the prehydrolyzed solution was mixed with the emulsion and reacted to make silica nanocapsules. For both 6-hour and 10-hour pre-hydrolyzed TEOS, silica nanocapsules still formed with similar size and good monodispersity (**Fig. 10**). However, 18-hour pre-hydrolysis resulted in the formation of big aggregates, because silica nuclei already formed after such a long hydrolysis time. Consequently, mixing of the positively charged emulsion and negatived charged silica nuclei led to instant aggregation.

Table 3. Size and zeta potential for prehydrolysed silica capsules

Pre-hydrolysis time (hours)	**Z-Ave (d.nm)**	**PDI**	**ZP (mV)**
6	259±8	0.24±0.01	30±3
10	230±6	0.17±0.02	40±2

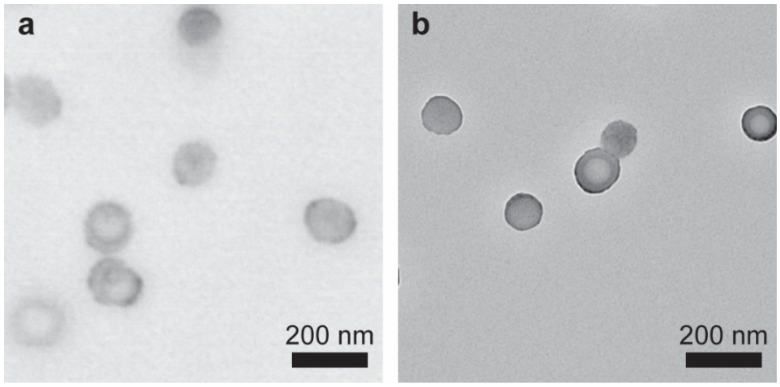

Fig. 11 Silica nanocapsule formation using pre-hydrolyzed TEOS. **a.** 6 hours prehydrolysis; **b.** 10 hours prehydrolysis. The scale bars are 200 nm.

Mechanism of interface-peptide mediated silica nanocapsule formation

Based on the systematic study above on all the key factors affecting nanocapsule formation, we propose a mechanism for the interface-peptide mediated silica nanocapsule formation (**Fig. 11).** Positively charged SurSi peptide adsorbs on the emulsion surface to stabilize the nanoemulsion. Upon the addition of a silica precursor TEOS, hydrolysis of TEOS starts. The concentration of hydrolyzed silicic acid and silicate oligomers increases with the concentrations of TEOS. When the concentration of silicate oligomers rises to the critical heterogamous nucleation concentration (C1), nucleation occurs at the peptide-covered oil-water interface and large amount of oligomers are consumed (**Fig. 11a**). However, when the concentration of silicate oligomers is higher than a critical homogenous nucleation concentration in bulk solution (C2), silica nanoparticles start to form in bulk solution (**Fig. 11a**). Until the oligomer concentration is below C1, homogeneous nucleation terminates while heterogeneous nucleation starts, thus leading to the formation of both silica nanoparticles and silica nanocapsules. Therefore, to avoid forming silica nanoparticles in bulk solution, the oligomer concentration needs to be below C2 but above C1 (**Fig. 11a**). A number of amino acids in SurSi play important roles in peptide-mediated biosilicification (**Fig. 11b**). Four amino acid residues including serine (S), tyrosine (Y), histidine (H) and glutamine (Q) are able to promote nucleophilic attack thus facilitating the hydrolysis of TEOS. Additionally, Serine (S) and tyrosine (Y) enhance the formation of hydrogen bonding with silanol while positively charged lysine (K) and arginine (R) interact with negative silanolate through electrostatic interaction or ion pairing. As a result, the concentrations of TEOS and SurSi should be within a proper range. Under such conditions, negatively charged silicate oligomers are attracted to the emulsion droplet surface by electrostatic interaction and condensed to form a layer of silica

shell. Then more SurSi peptide adsorbs and induces more silica formation at the shell until SurSi or silicic acid is fully consumed (**Fig. 11c**), or the reaction is stopped by dialysis to remove residual SurSi and silicic acid in the bulk solution. The SurSi concentration in the bulk solution is critical, as high SurSi concentration promotes quick hydrolysis and condensation of TEOS and higher concentration of silicate oligomers, thus higher chance forming silica nanoparticles in the bulk solution. On the contrary, if the peptide concentration is too low, the biosilicification reaction occurs too slow. Therefore, the residual peptide concentration in the bulk solution should be controlled by tuning dialysis time. As demonstrated in our experiment, dialysis for 5-20 h is appropriate for forming uniform nanocapsules. After all the optimization experiments described above, the optimized conditions for forming silica nanocapsules using the SurSi peptide was obtained (400 μM SurSi to form nanoemulsion, 5-20 hours dialysis with pH=7.5 HEPES buffer, reacted with 40 mM TEOS).

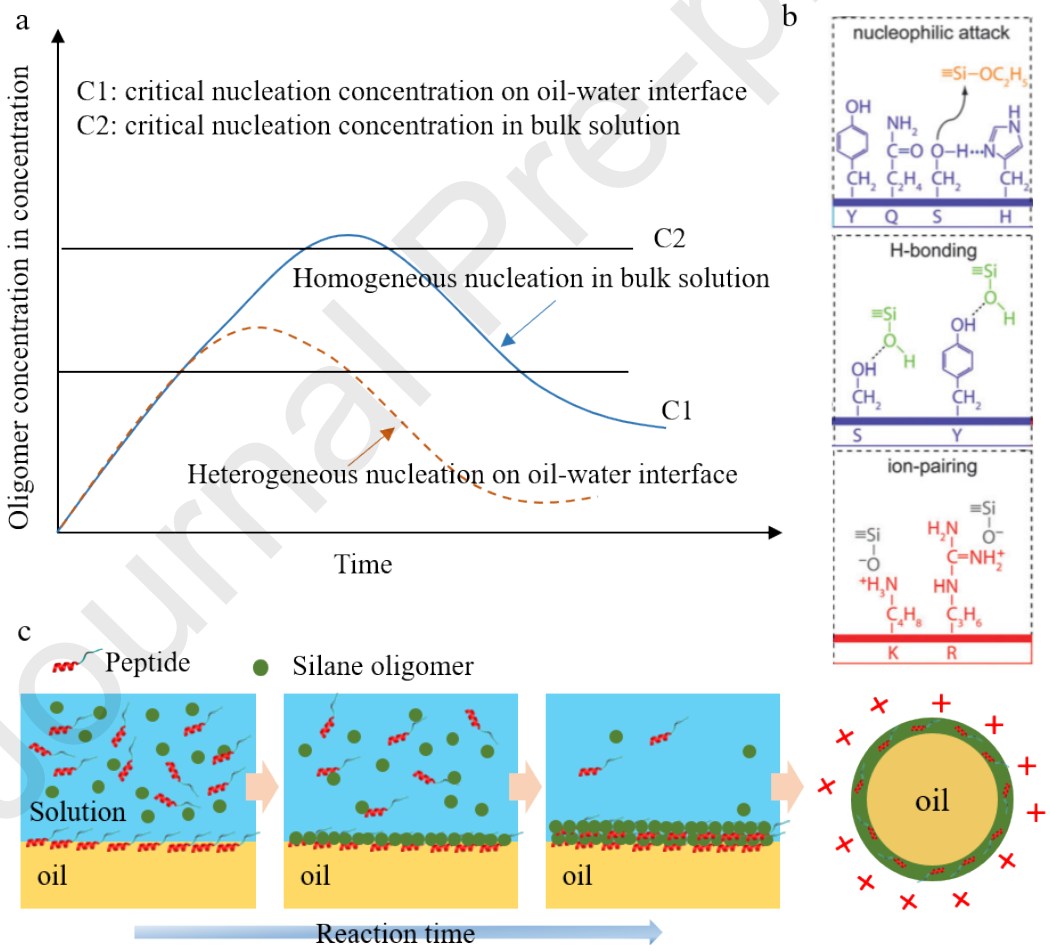

Fig. 12 Mechanism of interface-peptide mediated silica nanocapsule formation. **(a)** Schematic illustration of peptide/silicate oligomers concentration in the bulk solution at different reaction time in the presence of oil-water interfaces (emulsion droplets); **b.** Schematic illustration of

interface-kinetics mediated nucleation and silica growth thus the formation of oil-core silica-shell nanocapsules.

Conclusions

This study presents a fundamental study on the formation of core-shell silica nanocapsules using a dual-functional peptide SurSi, which is not only able to facilitate the formation of uniform nanoemulsions as a result of the surfactant module, but also induce biosilicification at oil-water interface forming silica shell because of its biosilicification activity. Several key factors affect the biosilicification at the oil-water interface thus forming uniform silica nanocapsules including silica precursor concentration, SurSi peptide concentration, and reaction pH. High silica precursor concentration, SurSi peptide and pH resulted in faster hydrolysis and biosilicification, thus forming uncontrolled silica formation in the bulk solution. Under optimized conditions (40 mM silica precursor TEOS, 400 μM SurSi, and pH 7.5), uniform silica nanocapsules of 150 nm were synthesized. SurSi peptide was found to play critical roles not only in the nucleation of silica at the oil-water interface but also the continuing growth of the silica shell. It took 18-20 hours for the hydrolysis of TEOS in the presence of SurSi peptide at pH 7.5 followed by nucleation and silica growth at the interface via a sol-gel process. Both the FTIR and TGA result confirmed that SurSi peptide was incorporated in the silica shell, thus resulting in a positive charge in contrast to the negatively charged silica formed using the traditional Stober method. Furthermore, to control the interface-peptide mediated biosilicification, SurSi concentration in the bulk solution is critical. Dialysis (5-20 h) is able to control SurSi concentration below the homogeneous nucleation in the bulk solution, but above the heterogeneous nucleation at the oil-water interface to form uniform silica nanocapsules. These fundamental understandings of the mechanism of interface peptide induced silica formation is essential to obtain oil-core silica-shell nanocapsules with well controlled properties. It also provides new insight into the design of new core-shell materials based on biomineralisation.

Acknowledgements

The project was supported by the Australian Research Council projects (FT140100726, DP150100798 and DP200101238). The authors acknowledge the facilities, and the scientific

and technical assistance, of the Australian Microscopy & Microanalysis Research Facility at the Centre for Microscopy and Microanalysis, The University of Queensland. This work was performed in part at the Queensland node of the Australian National Fabrication Facility. A company established under the National Collaborative Research Infrastructure Strategy to provide nano and microfabrication facilities for Australia's researchers.

Reference

[1] G. Yang, Y. Liu, S. Jin, C.X. Zhao, Development of Core-Shell Nanoparticle Drug Delivery Systems Based on Biomimetic Mineralization, Chembiochem 21 (2020) 1-10.
[2] R. Ghosh Chaudhuri, S. Paria, Core/Shell Nanoparticles: Classes, Properties, Synthesis Mechanisms, Characterization, and Applications, Chemical Reviews 112(4) (2012) 2373-2433.
[3] D. Wibowo, Y. Hui, A.P.J. Middelberg, C.X. Zhao, Interfacial engineering for silica nanocapsules, Advances in Colloid and Interface Science 236 (2016) 83-100.
[4] A. Imhof, Preparation and Characterization of Titania-Coated Polystyrene Spheres and Hollow Titania Shells, Langmuir 17(12) (2001) 3579-3585.
[5] M. Ocana, W.P. Hsu, E. Matijevic, Preparation and properties of uniform-coated colloidal particles. 6. Titania on zinc oxide, Langmuir 7(12) (1991) 2911-2916.
[6] G. Yang, Y. Liu, H. Wang, R. Wilson, Y. Hui, L. Yu, D. Wibowo, C. Zhang, A.K. Whittaker, A.P.J. Middelberg, C.X. Zhao, Bioinspired Core-Shell Nanoparticles for Hydrophobic Drug Delivery, Angew Chem Int Ed Engl 58 (2019) 14357-14364.
[7] P.A. Dresco, V.S. Zaitsev, R.J. Gambino, B. Chu, Preparation and Properties of Magnetite and Polymer Magnetite Nanoparticles, Langmuir 15(6) (1999) 1945-1951.
[8] H. Zou, S. Wu, J. Shen, Polymer/Silica Nanocomposites: Preparation, Characterization, Properties, and Applications, Chemical Reviews 108(9) (2008) 3893-3957.
[9] M. Okaniwa, Synthesis of poly(tetrafluoroethylene)/poly(butadiene) core-shell particles and their graft copolymerization, Journal of Applied Polymer Science 68(2) (1998) 185-190.
[10] Y. Liu, G. Yang, T. Baby, Tengjisi, D. Chen, D.A. Weitz, C.-X. Zhao, Stable polymer nanoparticles with exceptionally high drug loading by sequential nanoprecipitation, Angew Chem Int Ed Engl (2020) DOI: 10.1002/anie.201913539
[11] G. Hota, S.B. Idage, K.C. Khilar, Characterization of nano-sized CdS–Ag2S core-shell nanoparticles using XPS technique, Colloids and Surfaces A: Physicochemical and Engineering Aspects 293(1) (2007) 5-12.
[12] G. Hota, S. Jain, K.C. Khilar, Synthesis of CdS–Ag2S core-shell/composite nanoparticles using AOT/n-heptane/water microemulsions, Colloids and Surfaces A: Physicochemical and Engineering Aspects 232(2) (2004) 119-127.
[13] M.Y. Han, W. Huang, C.H. Chew, L.M. Gan, X.J. Zhang, W. Ji, Large Nonlinear Absorption in Coated Ag2S/CdS Nanoparticles by Inverse Microemulsion, The Journal of Physical Chemistry B 102(11) (1998) 1884-1887.
[14] T. Li, J. Moon, A.A. Morrone, J.J. Mecholsky, D.R. Talham, J.H. Adair, Preparation of Ag/SiO2 Nanosize Composites by a Reverse Micelle and Sol−Gel Technique, Langmuir 15(13) (1999) 4328-4334.
[15] C. Song, W. Yu, B. Zhao, H. Zhang, C. Tang, K. Sun, X. Wu, L. Dong, Y. Chen, Efficient fabrication and photocatalytic properties of TiO2 hollow spheres, Catalysis Communications 10(5) (2009) 650-654.

[16] D.B. Shenoy, A.A. Antipov, G.B. Sukhorukov, H. Möhwald, Layer-by-Layer Engineering of Biocompatible, Decomposable Core−Shell Structures, Biomacromolecules 4(2) (2003) 265-272.
[17] S. Srivastava, N.A. Kotov, Composite Layer-by-Layer (LBL) Assembly with Inorganic Nanoparticles and Nanowires, Accounts of Chemical Research 41(12) (2008) 1831-1841.
[18] L. Zhang, M. D'Acunzi, M. Kappl, G.K. Auernhammer, D. Vollmer, C.M. van Kats, A. van Blaaderen, Hollow Silica Spheres: Synthesis and Mechanical Properties, Langmuir 25(5) (2009) 2711-2717.
[19] C.X. Zhao, L. Yu, A.P.J. Middelberg, Magnetic mesoporous silica nanoparticles end-capped with hydroxyapatite for pH-responsive drug release, Journal of Materials Chemistry B 1(37) (2013) 4828-4833.
[20] C.-X. Zhao, L. Yu, A.P.J. Middelberg, Design of low-charge peptide sequences for high-yield formation of titania nanoparticles, Rsc Advances 2(4) (2012) 1292-1295.
[21] D. Zou, L. Yu, Q. Sun, Y. Hui, Tengjisi, Y. Liu, G. Yang, D. Wibowo, C.-X. Zhao, A general approach for biomimetic mineralization of MOF particles using biomolecules, Colloids and Surfaces B: Biointerfaces (2020) 111108.
[22] K. Liang, R. Ricco, C.M. Doherty, M.J. Styles, S. Bell, N. Kirby, S. Mudie, D. Haylock, A.J. Hill, C.J. Doonan, P. Falcaro, Biomimetic mineralization of metal-organic frameworks as protective coatings for biomacromolecules, Nat Commun 6 (2015) 7240.
[23] Y. Hui, X. Yi, D. Wibowo, G. Yang, A.P.J. Middelberg, H. Gao, C.-X. Zhao, Nanoparticle elasticity regulates phagocytosis and cancer cell uptake, Science Advances 6(16) (2020) eaaz4316.
[24] Y. Hui, D. Wibowo, Y. Liu, R. Ran, H.F. Wang, A. Seth, A.P.J. Middelberg, C.X. Zhao, Understanding the Effects of Nanocapsular Mechanical Property on Passive and Active Tumor Targeting, Acs Nano 12(3) (2018) 2846-2857.
[25] G.Z. Yang, D. Wibowo, J.H. Yun, L.Z. Wang, A.P.J. Middelberg, C.X. Zhao, Biomimetic Silica Nanocapsules for Tunable Sustained Release and Cargo Protection, Langmuir 33(23) (2017) 5777-5785.
[26] Y. Hui, D. Wibowo, C.X. Zhao, Insights into the Role of Biomineralizing Peptide Surfactants on Making Nanoemulsion-Templated Silica Nanocapsules, Langmuir 32(3) (2016) 822-830.
[27] D. Wibowo, C.X. Zhao, A.P.J. Middelberg, Interfacial Biomimetic Synthesis of Silica Nanocapsules Using a Recombinant Catalytic Modular Protein, Langmuir 31(6) (2015) 1999-2007.
[28] D. Wibowo, C.X. Zhao, B.C. Peters, A.P.J. Middelberg, Sustained Release of Fipronil Insecticide in Vitro and in Vivo from Biocompatible Silica Nanocapsules, Journal of Agricultural and Food Chemistry 62(52) (2014) 12504-12511.
[29] D. Wibowo, C.X. Zhao, A.P.J. Middelberg, Emulsion-templated silica nanocapsules formed using bio-inspired silicification, Chemical Communications 50(77) (2014) 11325-11328.
[30] H.F. Wang, D. Wibowo, Z. Shao, A.P.J. Middelberg, C.X. Zhao, Design of Modular Peptide Surfactants and Their Surface Activity, Langmuir 33(32) (2017) 7957-7967.
[31] W. Stöber, A. Fink, E. Bohn, Controlled growth of monodisperse silica spheres in the micron size range, Journal of Colloid and Interface Science 26(1) (1968) 62-69.
[32] V.K. LaMer, R.H. Dinegar, Theory, Production and Mechanism of Formation of Monodispersed Hydrosols, Journal of the American Chemical Society 72(11) (1950) 4847-4854.
[33] S. Yoon, B. Lee, C. Kim, J.H. Lee, Controlled Heterogeneous Nucleation for Synthesis of Uniform Mesoporous Silica-Coated Gold Nanorods with Tailorable Rotational Diffusion and 1 nm-Scale Size Tunability, Crystal Growth & Design 18(8) (2018) 4731-4736.

[34] U. Schubert, Chemistry and Fundamentals of the Sol–Gel Process, in: D.L.a.M. Zayat (Ed.), The Sol–Gel Handbook: Synthesis, Characterization, and Applications, Wiley-VCH Verlag GmbH & Co. KGaA2015.